

Supplementary Information

Facile Phase and Composition Tuned Synthesis of Tin Chalcogenide Nanocrystals

Hyung Soon Im, Yoon Myung, Yong Jae Cho, Chang Hyun Kim, Han Sung Kim, Seung Hyuk Back, Chan Su Jung, Dong Myung Jang, Young Rok Lim, Jeunghee Park, and Jae-Pyoung Ahn

Table S1. Experimental condition for the synthesis of NCs. (*NA = not applicable)

	Pressure (Torr)			Annealing or reduction
	Sn(CH ₃) ₄	H ₂ S	Se(CH ₃) ₂	
Sn	30	0	0	NA*
Sn-SnS	30	15	0	NA
SnS	30	60	0	NA
SnS-Sn ₂ S ₃ -SnS ₂	30	120	0	NA
Sn ₂ S ₃ -SnS ₂	20	200	0	NA
SnS ₂	20	200	0	Annealing at 300 °C under Ar flow
SnS-Sn ₂ S ₃	20	200	0	Reduction at 300 °C under H ₂ flow
SnS-SnS ₂	20	200	0	Reduction at 350 °C under H ₂ flow
SnSe	30	0	60	NA
SnSe ₂	30	0	120	NA
SnSe-SnSe ₂	30	0	120	Reduction at 450 °C under H ₂ flow
SnS _{0.9} Se _{0.1}	30	30	3	NA
SnS _{0.7} Se _{0.3}	30	30	5	NA
SnS _{0.6} Se _{0.4}	30	30	10	NA
SnS _{0.4} Se _{0.6}	30	30	15	NA
SnS _{0.3} Se _{0.7}	30	23	17	NA
SnS _{0.1} Se _{0.9}	30	30	30	NA
SnSSe	20	200	50	Annealing at 300 °C under Ar flow

Fig. S1 A plot of the S composition (x) of $\text{SnS}_x\text{Se}_{1-x}$ NCs versus that of $[\text{H}_2\text{S}]_x[\text{DMS}]_{1-x}$.

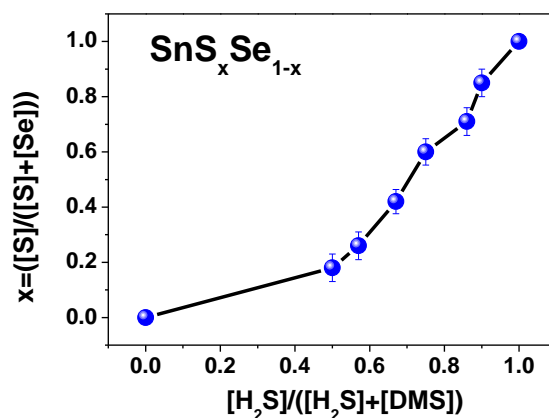


Fig. S2 (a) HRTEM image of SnSe-SnSe_2 hybrid. (b) The d -spacing of the (001) planes of SnSe_2 was clearly identified as 6.2 Å, from the intensity line profiles over the selected area at the edge of the nanosheets, which is consistent with those of the bulk. (c) The adjacent O-phase SnSe and H-phase SnSe_2 domains were identified by the corresponding FFT images (insets). The (111) planes of SnSe ($d_{111} = 3.0$ Å) and the (001) planes of SnSe_2 ($d_{001} = 6.2$ Å) were confirmed.

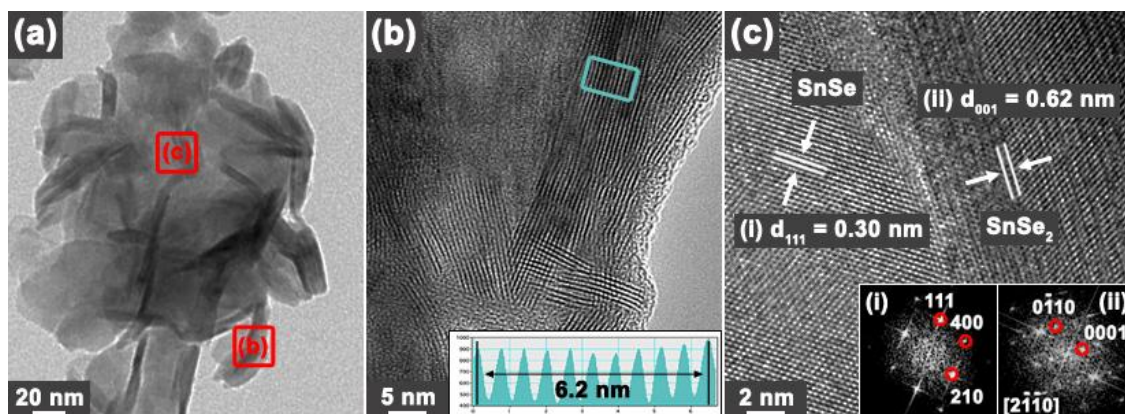


Fig. S3 HRTEM and FFT images of (a) O-phase $\text{SnS}_{0.4}\text{Se}_{0.6}$ and (b) H-phase SnSSe . The d -spacing of the (111) planes of $\text{SnS}_{0.4}\text{Se}_{0.6}$ NCs was 2.9 Å, corresponding to that of the bulk; c.f. $d_{111}=2.8$ Å (SnS) and 3.0 Å (SnSe). The EDX data (Sn L, S K, and Se L shells) confirmed an atomic ratio of Sn:S:Se = 1:0.4:0.6. Line-scanned data showed that Sn, S, and Se in ratios of 1:0.4:0.6 distributed homogeneously along the cross-section of the NCs. The d -spacing of the (001) planes of SnSSe nanosheets was clearly identified as 6.0 Å, from the intensity line profiles, which is consistent with those of the bulk; c.f. $d_{001}=5.9$ Å (SnS_2) and 6.2 Å (SnSe_2). EDX data showed their corresponding compositions Sn:S:Se=1:1:1.

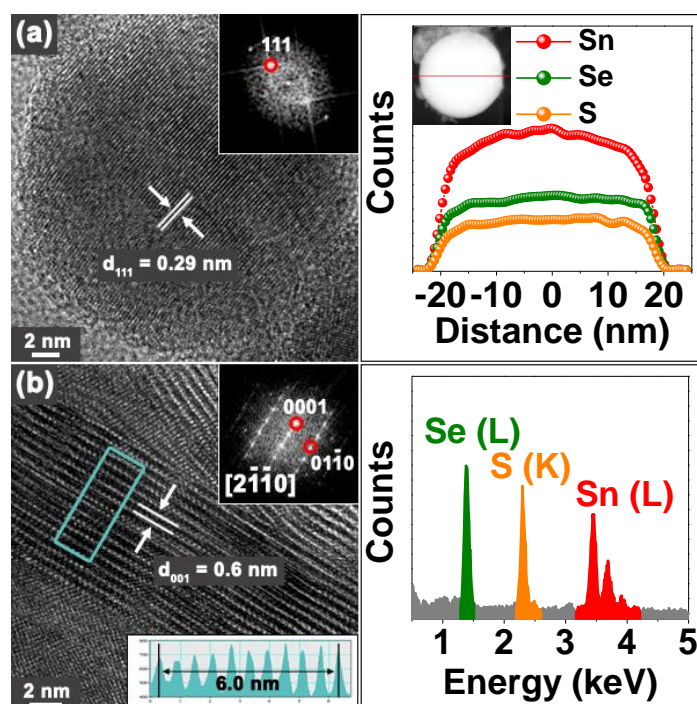


Fig. S4 UV-visible-NIR absorption spectra of (a) SnS, $\text{SnS}_{0.4}\text{Se}_{0.6}$, and SnSe; (b) SnS_2 , SnSSe, and SnSe_2 ; (c) Sn_2S_3 - SnS_2 NCs. The spectra were used to estimate the indirect and direct band gaps by performing Kubelka-Munk transformations [Reference: A. Hagfeldt, and M. Grätzel, *Chem. Rev.* 1995, **95**, 49-68.]. A plot of $[ah\nu]^2$ and $[ah\nu]^{1/2}$

(where α is the absorption coefficient) versus photon energy yielded the direct and indirect band gaps, respectively. The value is listed in Table S1.

For SnS, SnS_{0.4}Se_{0.6}, and SnSe, the optical band gaps were estimated to be 1.24 eV (1000 nm), 1.06 eV (1170 nm), and 0.96 eV (1290 nm), from the onset of absorption band, which is consistent with the indirect band gap. These values also agree with those determined in previous studies on NCs; E_g (SnS) = 1.1 eV (diameter = 3 nm), 1.27 eV (diameter = 280 nm); E_g (SnSe) = 0.9 eV (diameter = 9 nm), 1.15 eV (diameter = 4.5 nm), 1.12 eV (nanowires) [References are 1, 10, 13, 20, and 21 of the text].

The optical band gaps were 2.26 eV (549 nm), 1.70 eV (726 nm), and 1.14 eV (1088 nm), for SnS₂, SnSSe, and SnSe₂, respectively, from the onset of absorption band. The values of SnS₂ and SnSSe are close to the direct band gap, while that of SnSe₂ is rather close to the indirect band gap. The band gap of SnS₂ NCs agrees with the value of previous works; 2.25~2.32 eV (diameter = ~20 nm) [Reference: Y. C. Zhang, J. Li, M. Zhang and D. D. Dionysiou, *Environ. Sci. Technol.* 2011, **45**, 9324-9331.], and 2.23 eV (single sheet) [Reference: Y. Sun, H. Chen, S. Gao, Z. Sun, Q. Liu, Q. Liu, F. Lei, T. Yao, J. He, S. Wei and Y. Xie, *Angew. Chem. Int. Ed.* 2012, **51**, 8727-8731.].

The optical band gap (direct) of Sn₂S₃ was estimated to be 1.24 eV (1000 nm) from the onset of the spectrum of Sn₂S₃-SnS₂, since the band gap of SnS₂ is 2.3 eV. Previous works showed that Sn₂S₃ is a mixed Sn (II)-Sn (IV) valence compound semiconductor, and the band gap depends strongly on the crystalline structure and stoichiometry, over the wide range of 0.95~2.2 eV; E_g = 0.95 eV [Reference: U. V. Alpen, J. Penner and E. Gmelin, *Mat. Res. Bull.*, 1975, **10**, 175-180.]; 1.16 eV [Reference: S. Lopez, S.

Granados and A. Ortiz, *Semicond. Sci. Technol.*, 1996, **11**, 433-436.]; 1.9-2.2 eV (indirect) [Reference: H. Ben Haj Salah, H. Bouzouita and B. Benzig, *Thin Solid Films* 2005, **480**, 439-442.]; 2.0 eV (direct) [Reference: M. Khadraoui, N. Benramdane, C. Mathieu, A. Bouzidi, R. Milou, Z. Kebbab, K. Sahraoui and R. Desfeux. *Solid Stat. Commun.* 2010, **150**, 297-300.]; 1.2 and 1.57 eV (direct) [Reference: A. J. Ragina, K. V. Murail, K. C. Preetha, K. Deepa and T. L. Remadevi, *J. Mater. Sci.: Mater. Electron.*, 2012, **23**, 2264-2271.].

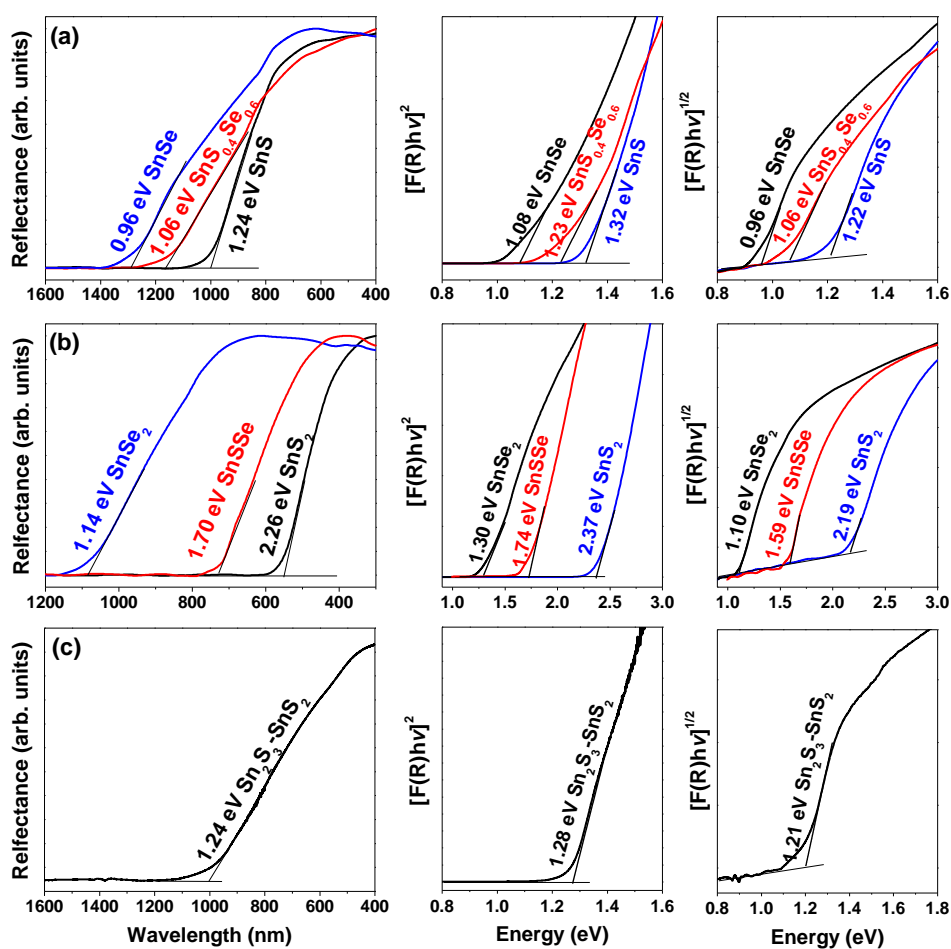


Table S2. Optical band gap (from the onset of absorption spectrum), and direct/indirect band gaps, estimated using Kubelka-Munk transformations.

	E_g from the onset (eV)	E_g (direct)	E_g (indirect)
SnS	1.24	1.32	1.22
SnS _{0.4} Se _{0.6}	1.06	1.23	1.06
SnSe	0.96	1.08	0.96
SnS ₂	2.26	2.37	2.19
SnSSe	1.70	1.74	1.59
SnSe ₂	1.14	1.30	1.10
Sn ₂ S ₃ -SnS ₂	1.24	1.28	1.21

Fig. S5 The CV data were measured using an electrochemical analyzer (IVIUM CompactStat) using gold (area ca. 0.02 cm²) disks as the working electrode, a Pt-wire auxiliary electrode and an Ag/0.01 M AgNO₃ reference electrode (BAS Inc., 0.1 M tetrabutylammonium hexafluorophosphate (TBAPF₆)/ acetonitrile electrolyte).

(a) CV curves (vs. Ag/Ag⁺ reference electrode) of SnS, SnS_{0.4}Se_{0.6}, and SnSe, recorded at a scan rate of 20 mVs⁻¹, showing strong oxidation peaks (E_{Ox}) and weak reduction peaks (E_{Red}). The valence band (VB) and conduction band (CB) energies of NCs were calculated from the E_{Ox} and E_{Red} values, assuming the energy level of ferrocene/ferrocenium (Fc/Fc⁺) to be -4.8 eV below the vacuum level. The formal potential of Fc/Fc⁺ was measured to be 0.085 V against an Ag/Ag⁺ reference electrode. Therefore, E_{VB} (E_{HOMO}) = $-(E_{Ox}+4.715)$ eV; E_{CB} (E_{LUMO}) = $-(E_{Red}+4.715)$ eV, where the onset potential values are relative to the Ag/Ag⁺ reference electrode. From the onset value of E_{Ox} peak (~0.4 V), the position of the valence band (VB) edge was estimated to be $E_{VB} = -5.2$ eV from the vacuum level. The weak reduction peaks (E_{Red}) appeared at nearly the same voltage (onset at -0.9 V), suggesting $E_{CB} = -3.8$ eV from vacuum level. Taken the E_{VB} (which is more reliable due to the well-defined peak shape) and the

optical band gap (from the UV-Vis-NIR absorption spectrum), $E_{CB} = -4.0, -4.1, \text{ and } -4.2$ eV were obtained. Table S2 summarizes the results.

(b) CV curves of SnS₂, SnSSe, and SnSe₂ NCs at a scan rate of 20 mVs⁻¹ show the oxidation peaks with onsets of 1.6, 1.1, and 0.7 V, respectively. From this onset value, the positions of the VBs were estimated to be $E_{VB} = -6.3, -5.8, \text{ and } -5.4$ eV, respectively. Taken these E_{VB} values and the optical band gap (from the UV-Vis-NIR absorption spectrum), $E_{CB} = -4.0, -4.1, \text{ and } 4.3$ eV were obtained. The E_{CB} values were coherently obtained using the reduction peaks. The E_{VB} and E_{CB} values are close to the work function (Φ) and electron affinity (χ) of the bulk: $\Phi = 6.3$ eV and $\chi = 4.2$ eV for SnS₂; $\Phi = 5.35$ eV and $\chi = 4.4$ eV for SnSe₂ [Reference: R. H. Williams, R. B. Murray, D. W. Govan, J. M. Thomas and E. L. Evans, *J. Phys. C: Solid State Phys.*, 1973, **6**, 3631-3642].

(c) CV curves of Sn₂S₃-SnS₂ and SnS-Sn₂S₃ NCs at a scan rate of 20 mVs⁻¹. The Sn₂S₃-SnS₂ show two oxidation peaks with onsets of 1.0 and 1.6 V, which can be assigned to Sn₂S₃ and SnS₂, respectively. The SnS-Sn₂S₃ also show two oxidation peaks with onsets of 0.4 and 1.0 V, which can be assigned to SnS and Sn₂S₃, respectively. There are two reduction peaks with onsets of -0.3 and -0.9 V, which can be assigned to Sn₂S₃ and SnS, respectively. From the same onset value of E_{Ox} peaks (1.0 V), the VB position of Sn₂S₃ was estimated to be $E_{VB} = -5.7$ eV. Using this E_{VB} value and the optical band gap (1.24 eV) from the UV-Vis-NIR absorption spectrum), $E_{CB} = -4.5$ eV were obtained. The E_{VB} value is consistent with the value estimated using $E_{Red} = -0.3$ V.

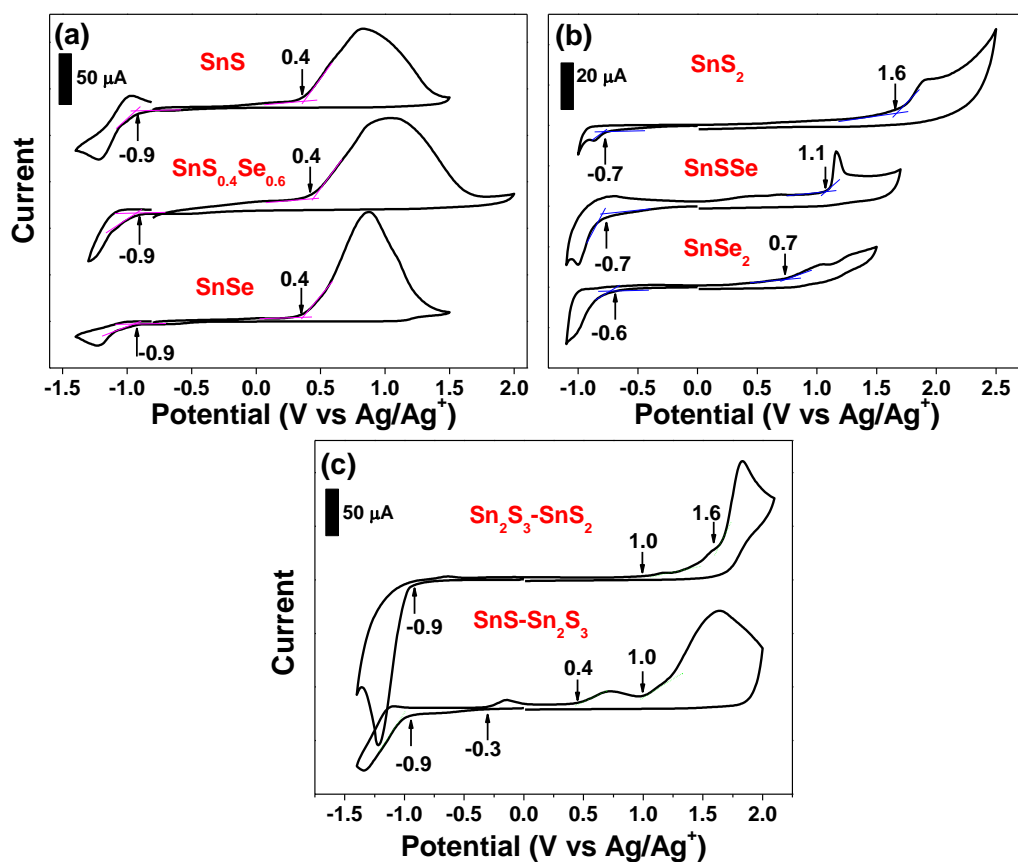


Table S3. Position of conduction and valence bands (in eV) versus vacuum level, which were estimated from the CV and UV-Vis-NIR absorption spectroscopy data.

	E_{Ox} (V)	E_{Red} (V)	$E_{Ox}-E_{Red}$ (V)	E_{VB} (eV) ^a	E_{CB} (eV) ^b	E_g (eV) ^c	E_{CB} (eV) ^d
SnS	0.4	-0.9	1.3	-5.1	-3.8	1.24	-3.9
SnS _{0.4} Se _{0.6}	0.4	-0.9	1.3	-5.1	-3.8	1.06	-4.0
SnSe	0.4	-0.9	1.3	-5.1	-3.8	0.96	-4.1
SnS ₂	1.6	-0.7	2.3	-6.3	-4.0	2.26	-4.0
SnSSe	1.1	-0.7	1.8	-5.8	-4.0	1.70	-4.1
SnSe ₂	0.7	-0.6	1.3	-5.4	-4.1	1.14	-4.3
Sn ₂ S ₃	1.0	-0.3	1.3	-5.7	-4.4	1.24	-4.5

^a $E_{VB} = -(E_{Ox} + 4.715)$ eV; ^b $E_{CB} = -(E_{Red} + 4.715)$ eV; ^cOptical band gap, which is estimated from the UV-visible-NIR absorption spectrum; ^d E_{CB} (eV) = $E_{VB} + E_g$ (optical band gap)